Published in IET Signal Processing
Received on 23rd May 2008
Revised on 11th December 2008
doi: 10.1049/iet-spr.2008.0094

ISSN 1751-9675

Digital fractional order operators for R-wave detection in electrocardiogram signal

M. Benmalek A. Charef

Laboratoire de Traitement du Signal Département d'Electronique Université, Mentouri de Constantine Route Ain El-Bey, Constantine 25000, Algeria
E-mail: afcharef@yahoo.com

Abstract: In this study, we present an effective R-wave detection method in the QRS complex of the electrocardiogram (ECG) based on digital differentiation and integration of fractional order. The detection algorithm is performed in two steps. The pre-processing step is based on a fractional order digital band-pass filter whose fractional order is obtained by maximising the signal to noise ratio of the ECG signal, followed by a five points differentiator of fractional order 1.5 then the squaring transformation and the smoothing are used to generate peaks corresponding to the ECG parts with high slopes. The detection step is a new and simple strategy which is also based on fractional order operators for the localisation of the R waves. The MIT/BIH arrhythmia database is used to test the effectiveness of the proposed method. The algorithm has provided very good performance and has achieved about 99.86% of the detection rate for the standard database. The results obtained are presented, discussed and compared to the most recent and efficient R-wave detection algorithms.

1 Introduction

The electrocardiogram (ECG) provides important information on the condition of the heart of a patient. R-wave detectors are extremely useful tools in any automatic ECG signal analysis system for finding fiduciary points, averaging methods, calculating the RR time series in heart rate variability, examining the ST-segment, compressing the ECG, and classifying the ECG waveform. The time-varying morphology of ECG, the physiological variability of the QRS complexes along with the noise contamination from various sources, including power-line interference, muscle contraction, poor electrode contact, patient movement artefacts, baseline wandering due to respiration and saturation of the amplifiers, increase the difficulty of the QRS complex detection task [1]. P and T waves with large amplitudes can also be confused with QRS complexes [1]. Although a large number of QRS complex detection methods have so far been reported [2–8], a perfect algorithm which is sufficiently reliable in a strictly practical sense has not been developed; therefore, research work is still underway in many aspects towards the enhancement of QRS detection.

In the last decades considerable focus on fractional derivatives has been simulated by their applications in different areas of physics and engineering [8–13]. Only in recent years can one find some applications in signal processing theory [3, 14–16]. The interest for the introduction of these concepts in signal processing applications has been motivated by their good performances and robustness obtained in control theory. Also, the generalisation from integer orders to fractional orders in derivatives and integrals gives rise to more flexibility in designing signal processing algorithms and systems [17, 18].

In this paper, we present a novel method for the QRS detection algorithm, which uses digital fractional order integration and differentiation. The proposed method is divided into two major parts. The first part is ECG pre-processing, which is based on a digital band-pass filter whose fractional order is obtained by maximising the signal to noise ratio (SNR) of the ECG signal, followed by a five points differentiator of fractional order 1.5, and then by the squaring transformation and the smoothing to generate peaks corresponding to the ECG parts with high slopes. The second part is the detection step, which is also based

on digital fractional order differentiators. R-wave localisation is performed by a new and simple strategy that is built using two digital fractional order differentiators of order α and 2α such that $0.5 < \alpha < 1$. The MIT/BIH arrhythmia database was used to test the effectiveness of the proposed method. The results obtained are presented, discussed and compared to the most recent and efficient R-wave detection algorithms. The proposed technique offers performance comparable to the best existing methods in the literature [2–8].

We believe that the use of fractional order operators is a very promising technique for ECG analysis because, in contrast to integer order operators, in which derivatives depend only on the local behaviour of the function, fractional order operators accumulate the whole information of the function in a weighted form.

2 Digital fractional order integrator and differentiator

This section deals with the digital modelling of the fractional order differentiator s^m and integrator s^{-m} for $0 < m < 1$. The proposed approach is based on Charef's analogue approximation of these operators [19, 20]. The differentiator and integrator expressed as rational discrete transfer functions are obtained by the discretisation of their rational analogue transfer functions using Euler's generating function $s = (1 - z^{-1})/T$ [21] in a given frequency band of practical interest. The coefficients of these discrete transfer functions are given in closed form in terms of the sampling period T and the approximation parameters.

The analogue fractional order integrator and differentiator are represented by the following irrational transfer function, respectively

$$G_{\mathrm{I}}(s) = \frac{1}{s^m} \quad \text{for } 0 < m < 1 \tag{1}$$

$$G_{\mathrm{D}}(s) = s^m \quad \text{for } 0 < m < 1 \tag{2}$$

In a given frequency band of interest (ω_{L}, ω_{H}), (1) and (2) can be approximated by a rational transfer function as follows

$$G_{\mathrm{I}}(s) = \frac{1}{s^m} \cong K_{\mathrm{I}} \frac{\prod_{i=0}^{N-1}(1 + s/z_{\mathrm{I}i})}{\prod_{i=0}^{N}(1 + s/p_{\mathrm{I}i})} = \sum_{i=0}^{N} \frac{k_{\mathrm{I}i}}{(1 + s/p_{\mathrm{I}i})} \tag{3}$$

$$G_{\mathrm{D}}(s) = s^m \cong K_{\mathrm{D}} \frac{\prod_{i=0}^{N}(1 + s/z_{\mathrm{D}i})}{\prod_{i=0}^{N}(1 + s/p_{\mathrm{D}i})} = K_{\mathrm{D}} + \sum_{i=0}^{N} \frac{k_{\mathrm{D}i}}{(1 + s/p_{\mathrm{D}i})} \tag{4}$$

Poles $p_{\mathrm{I}i}$ and $p_{\mathrm{D}i}$, zeros $z_{\mathrm{I}i}$ and $z_{\mathrm{D}i}$, residues $k_{\mathrm{I}i}$ and $k_{\mathrm{D}i}$, and constants K_{I}, K_{D} and N of the above approximations are given in [19].

The IIR digital fractional order integrator and differentiator transfer functions are obtained by using Euler's generating function $s = (1 - z^{-1})/T$ (T is the sampling period) in (3) and (4), respectively, as

$$G_{\mathrm{I}}(z) = K_{\mathrm{I}} \frac{\prod_{i=0}^{N-1}[1 + \{(1 - z^{-1})/T\}/z_{\mathrm{I}i}]}{\prod_{i=0}^{N}[1 + \{(1 - z^{-1})/T\}/p_{\mathrm{I}i}]} = \sum_{i=0}^{N} \frac{k_{Ii}}{[1 + \{(1 - z^{-1})/T\}/p_{\mathrm{I}i}]} \tag{5}$$

$$G_{\mathrm{D}}(z) = K_{\mathrm{D}} \frac{\prod_{i=0}^{N}[1 + \{(1 - z^{-1})/T\}/z_{\mathrm{D}i}]}{\prod_{i=0}^{N}[1 + \{(1 - z^{-1})/T\}/p_{\mathrm{D}i}]} = K_{\mathrm{D}} + \sum_{i=0}^{N} \frac{k_{Di}}{[1 + \{(1 - z^{-1})/T\}/p_{\mathrm{D}i}]} \tag{6}$$

We have tested the Euler and Tustin transformation methods [22] and found that there was no big difference in our final detection results. So, we have chosen Euler's transformation because the derived equations are simpler. Besides, we know that the Euler analogue to digital discrete transformation produces a stable discrete time filter for a stable continuous filter [21]; hence the above IIR digital fractional order integrator and differentiator transfer functions are stable IIR filters because they are derived from stable continuous time filters of (3) and (4), respectively, using Euler's transformation.

Simplified forms of the above equations can be given as follows

$$G_{\mathrm{I}}(z) = \bar{K}_I \frac{\prod_{i=0}^{N-1}(z - \bar{z}_{\mathrm{I}i})}{\prod_{i=0}^{N}(z - \bar{p}_{\mathrm{I}i})} = \sum_{i=0}^{N} \frac{\bar{k}_{\mathrm{I}i} z}{(z - \bar{p}_{\mathrm{I}i})} \tag{7}$$

$$G_{\mathrm{D}}(z) = \bar{K}_{\mathrm{D}} \frac{\prod_{i=0}^{N}(z - \bar{z}_{\mathrm{D}i})}{\prod_{i=0}^{N}(z - \bar{p}_{\mathrm{D}i})} = \bar{K}_{\mathrm{D}} + \sum_{i=0}^{N} \frac{\bar{k}_{\mathrm{D}i} z}{(z - \bar{p}_{\mathrm{D}i})} \tag{8}$$

Poles $\bar{p}_{\mathrm{I}i}$ and $\bar{p}_{\mathrm{D}i}$, zeros $\bar{z}_{\mathrm{I}i}$ and $\bar{z}_{\mathrm{D}i}$, gains $\bar{K}_{\mathrm{I}}$ and $\bar{K}_{\mathrm{D}}$, and residues $\bar{k}_{\mathrm{I}i}$ and $\bar{k}_{\mathrm{D}i}$ can be easily calculated. The left hand of (7) and (8) can be rewritten as

$$G_{\mathrm{I}}(z) = \bar{K}_{\mathrm{I}} \frac{\prod_{i=0}^{N-1}(z - \bar{z}_{\mathrm{I}i})}{\prod_{i=0}^{N}(z - \bar{p}_{\mathrm{I}i})} = \frac{\sum_{i=0}^{N} \beta_{\mathrm{I}i} z^{i-(N+1)}}{1 + \sum_{i=0}^{N} \alpha_{\mathrm{I}i} z^{i-(N+1)}} \tag{9}$$

$$G_{\mathrm{D}}(z) = \bar{K}_{\mathrm{D}} \frac{\prod_{i=0}^{N}(z - \bar{z}_{\mathrm{D}i})}{\prod_{i=0}^{N}(z - \bar{p}_{\mathrm{D}i})} = \frac{\sum_{i=0}^{N+1} \beta_{\mathrm{D}i} z^{i-(N+1)}}{1 + \sum_{i=0}^{N} \alpha_{\mathrm{D}i} z^{i-(N+1)}} \tag{10}$$

where the coefficients $\alpha_{\mathrm{I}i}$, $\beta_{\mathrm{I}i}$ Z, $\alpha_{\mathrm{D}i}$, $\alpha_{\mathrm{I}i}$ and $\beta_{\mathrm{D}i}$ can also be easily obtained. Then the difference equations representing the digital fractional order integrator and differentiator are

doi: 10.1049/iet-spr.2008.0094

given respectively by

$$y_{\mathrm{I}}(k) = \sum_{i=0}^{N} \beta_{\mathrm{I}i} x[k-(N+1-i)] - \sum_{i=0}^{N} \alpha_{\mathrm{I}i} y_{\mathrm{I}}[k-(N+1-i)] \quad (11)$$

$$y_{\mathrm{D}}(k) = \sum_{i=0}^{N+1} \beta_{\mathrm{D}i} x[k-(N+1-i)] - \sum_{i=0}^{N} \alpha_{\mathrm{D}i} y_{\mathrm{D}}[k-(N+1-i)] \quad (12)$$

with $x(k)$ being the input and $y_{\mathrm{I}}(k)$ and $y_{\mathrm{D}}(k)$ the outputs of the digital fractional order integrator and differentiator, respectively. From (7) and (8), the impulse responses of these IIR digital fractional order integrator and differentiator can also be obtained as

$$g_{\mathrm{I}}(k) = \sum_{i=0}^{N} \bar{k}_{\mathrm{I}i} (\bar{p}_{\mathrm{I}i})^k \quad \text{for } k = 0, 1, \ldots, +\infty \quad (13)$$

$$g_{\mathrm{D}}(k) = \bar{K}_{\mathrm{D}} \delta(k) + \sum_{i=0}^{N} \bar{k}_{\mathrm{D}i} (\bar{p}_{\mathrm{D}i})^k \quad \text{for } k = 0, 1, \ldots, +\infty \quad (14)$$

By truncating the sequences $g_{\mathrm{I}}(k)$ and $g_{\mathrm{D}}(k)$ for $0 < k < (L-1)$, we obtain the FIR digital fractional order integrator and differentiator impulse responses of length L as

$$g_{\mathrm{IRIF}}(k) = \left\{ \begin{array}{ll} \frac{1}{M_{\mathrm{I}}} g_{\mathrm{I}}(k), & 0 \le k \le (L-1) \\ 0, & \text{otherwise} \end{array} \right\} \quad (15)$$

$$g_{\mathrm{DRIF}}(k) = \left\{ \begin{array}{ll} \frac{1}{M_{\mathrm{D}}} g_{\mathrm{D}}(k), & 0 \le k \le (L-1) \\ 0, & \text{otherwise} \end{array} \right\} \quad (16)$$

with $M_{\mathrm{I}} = \sum_{k=0}^{L-1} g_{\mathrm{I}}(k)$ and $M_{\mathrm{D}} = \sum_{k=0}^{L-1} g_{\mathrm{D}}(k)$ being normalisation parameters.

The bode plots of the fractional order integrator and differentiator transfer function and its digital implementation are shown in Figs. 1 and 2, respectively. As we are going to use these digital operators for the processing of the ECG signals of MIT/BIH database, the sampling period is thus taken as $T = 1/360$ s and the frequency band of practical interest for the approximation is $(\omega_{\mathrm{L}}, \omega_{\mathrm{H}}) = (2\pi \text{ rad/s}, 100\pi \text{ rad/s})$ because most of the energy of the QRS complex lies between 3 and 40 Hz [23]. The approximation band is deliberately chosen wider than the band of the signal in order to have a very good approximation of the fractional operators in the signal band.

The transfer function of a fractional order differentiator of fractional order $1 < m < 2$ can be written as

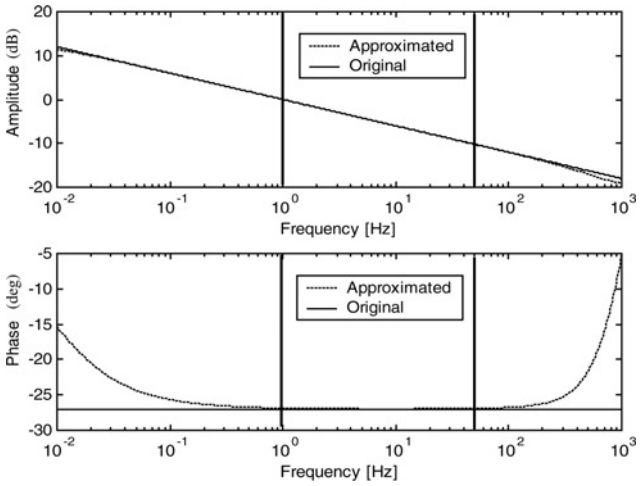

Figure 1 *Bode plots of the integrator $s^{-0.3}$ and its digital implementation*

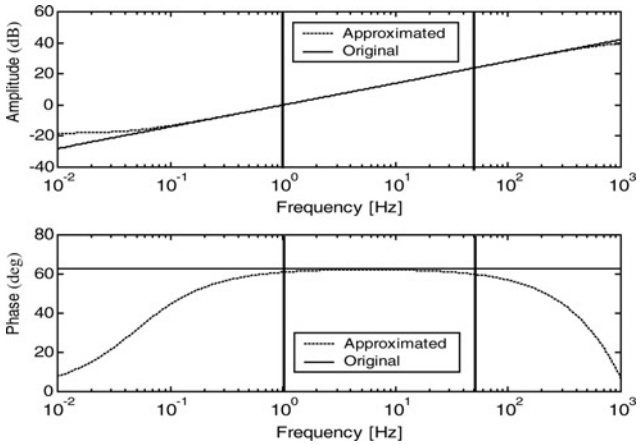

Figure 2 *Bode plots of the differentiator $s^{0.7}$ and its digital implementation*

$H_{\mathrm{D}}(s) = s^m = sG_{\mathrm{D}}(s)$, where $G_{\mathrm{D}}(s) = s^{(m-1)}$ such that $0 < (m-1) < 1$. The equivalent IIR digital fractional order differentiator of the analogue differentiator $H_{\mathrm{D}}(s)$ is

$$H_{\mathrm{D}}(z) = \frac{(1-z^{-1})}{T} G_{\mathrm{D}}(z) \quad (17)$$

In time domain, we will have

$$h_{\mathrm{D}}(k) = \frac{1}{T}\{g_{\mathrm{D}}(k) + g_{\mathrm{D}}(k-1)\} \quad (18)$$

3 ECG pre-processing design

ECG pre-processing is used to eliminate the P and T waves and various noises and also to enhance QRS complexes. Fig. 3 shows the different ECG pre-processing steps of the R-wave detection of the proposed algorithm.

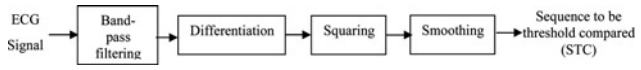

Figure 3 *Electrocardiogram preprocessing*

3.1 Band-pass filtering

Filtering is generally the first and most important step in ECG pre-processing. In this work we have introduced a new digital band-pass filter based on fractional order operators. The parameters (length and fractional order) of this filter are calculated to maximise the SNR of the ECG signal. As shown in Fig. 4, the introduced digital band-pass filter results from two cascaded filters. The first is a digital low-pass filter made up of a triangular filter in cascade with a fractional integrator of order m such that $0 < m < 1$. The second is a digital high-pass filter resulting from the difference of two branches in parallel; one of these branches is unity and the other branch is made up of a triangular filter cascaded with a fractional differentiator of the same order m as the fractional order integrator.

The triangular filter is formed by two cascaded moving average filters of period $L/2$, with L an even integer. Its impulse response $g_T(k)$ is such that [24]

$$g_T(k) = \begin{cases} \dfrac{4(k+1)}{L^2}, & 0 \le k \le \dfrac{L}{2} - 2 \\ \dfrac{4}{L} - \dfrac{4(k+1)}{L^2}, & \dfrac{L}{2} - 1 \le k \le (L-2) \\ 0, & \text{otherwise} \end{cases} \quad (19)$$

The digital fractional order integrator and differentiator outputs are, respectively, given as

$$y_I(k) = \sum_{i=0}^{L-1} g_{IRIF}(i)x(k-i) \quad (20)$$

$$y_D(k) = \sum_{i=0}^{L-1} g_{DRIF}(i)x(k-i) \quad (21)$$

where $g_{IRIF}(k)$ and $g_{DRIF}(k)$ are, respectively, the impulse responses of the digital fractional order integrator and differentiator as given by (15) and (16) and $x(k)$ is the input. The central frequency and the 3-dB bandwidth of this proposed digital filter are affected by the values of the fractional order m and the length L. So, the L and m values of the proposed filter are selected such that the SNR of the ECG signal is maximised using the following relation [25]

$$SNR_L(m) = \frac{E\{x(k)^2\}}{E[\{y_f(k) - x(k)\}^2]}, \quad k = 0, 1, \ldots, M \quad (22)$$

where $x(k)$ is the noisy ECG signal, $y_f(k)$, the output of the digital band-pass filter, is the ECG signal and $[y_f(k) - x(k)]$ is the noise, and $M+1$ is the number of samples. Figs. 5 and 6 show SNR as a function of length L with the fractional order m as a parameter for some records of the MIT/BIH database. The sampling rate of the ECG in the MIT/BIH database is 360 Hz, the parameter L is varied from 8 to 20 with a step of 2 and the parameter m is varied from 0.1 to 0.9 with a step of 0.01. From the results we found that the maximum $SNR_L(m)$ occurs for all the ECG records used at the same fractional order $m = 0.68$ but for different parameter L. This variation in length L for different ECG records may be due to the variations in QRS morphology and period width. With the fractional order $m = 0.68$, the amplitude frequency response and the impulse response of the proposed digital band-pass digital filter are given in Figs. 7 and 8, respectively, with length L as a parameter.

Table 1 contains the central frequency and the 3-dB bandwidth of this proposed digital band-pass filter. From this table we find that the central frequency is between 7 and 18 Hz and the 3-dB bandwidth is between 6 and 17 Hz. In [6, 26–29] the authors have stated that almost all R-wave detections based on digital filters use band-pass filters with central frequency between 10 and 25 Hz and the 3-dB bandwidth of this proposed band-pass filter is between 5 and 10 Hz.

In the literature, many researchers using wavelet techniques for R-wave detection have also found that the best detection results were obtained when the shape of the used smoothing prototype wavelet looks like the regular morphology of the QRS complex and this wavelet has a zero mean value. In our work, besides the fact that parameter $m = 0.68$ is obtained for the maximum SNR, we remark that all the shapes of the impulse responses of the digital band-pass filter for $m = 0.68$ and the different values of length L look like the regular morphology of the QRS complex. We have also found that each impulse response has almost a zero mean value. And the choice of the length L is based on the narrowest 3-dB bandwidth that corresponds, in our work, to $L = 20$.

We have used fractional order operators in the pre-processing for the following reasons:

1. It is now well known that many physical phenomena are modelled accurately and effectively using fractional derivatives, whereas the classical integer derivative-based models capture these phenomena only approximately.

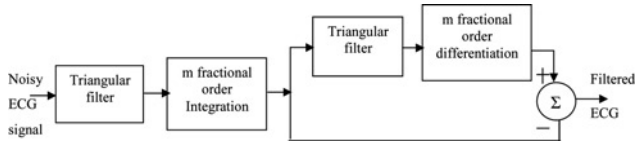

Figure 4 *Digital band-pass filter diagram*

doi: 10.1049/iet-spr.2008.0094

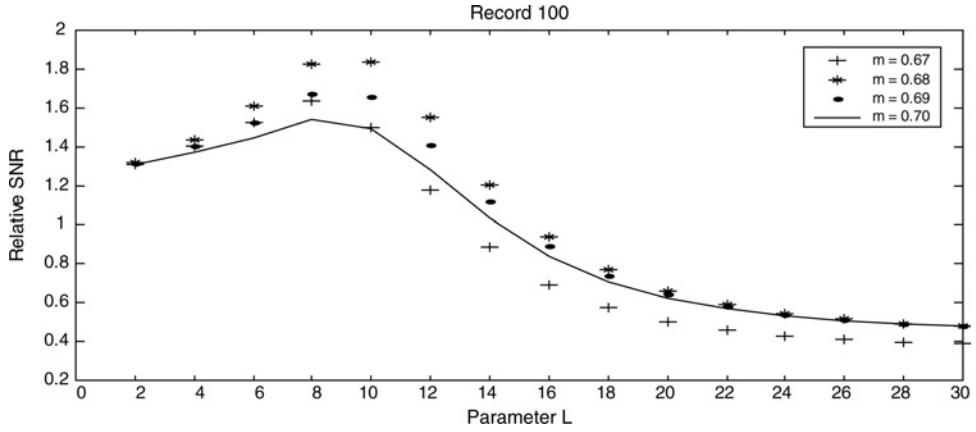

Figure 5 *SNR of record 100 versus L and different values of m*

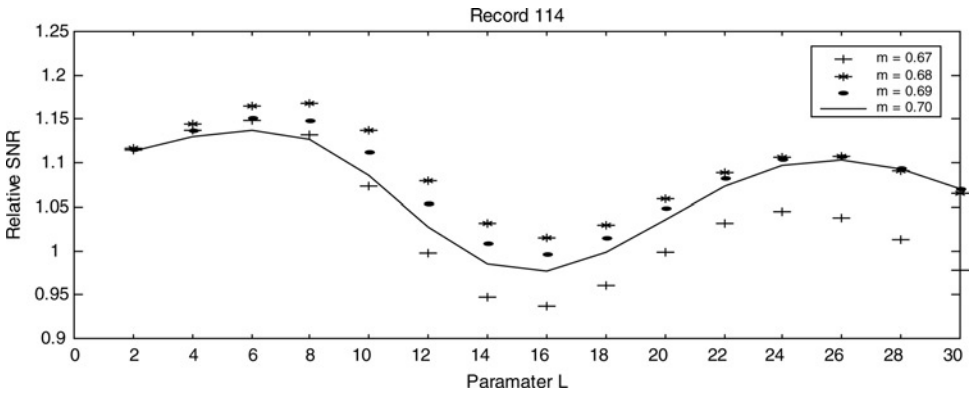

Figure 6 *SNR of record 114 versus L for different values of m*

2. The self-similar pattern of branching seen in the His-Purkinje conduction system of the heart has been studied by Goldberger *et al.* [30] by analysing a large number of QRS complexes for healthy adult males. They found that the plot of the power spectrum of these QRS complexes at different harmonics frequencies in log–log plot shows that it behaves as $1/f^{\beta}$, the inverse power law system. They also proved that the fractal-like nature of the His-Purkinje network serves as the structural substrate for the $1/f^{\beta}$ spectrum of the normal QRS complex. This

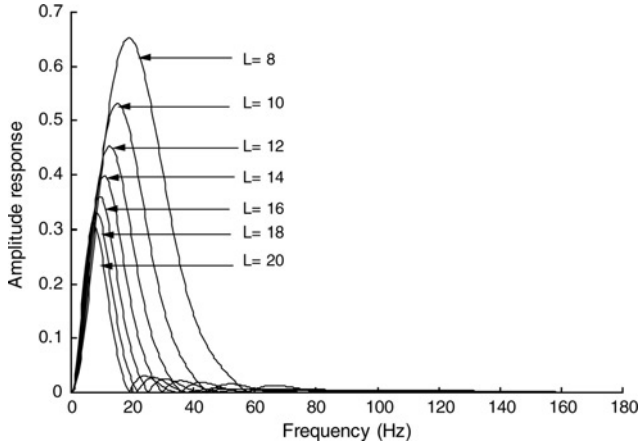

Figure 7 *Amplitude frequency responses of digital the band-pass filter for m = 0.68 and different values of L with m = 0.68*

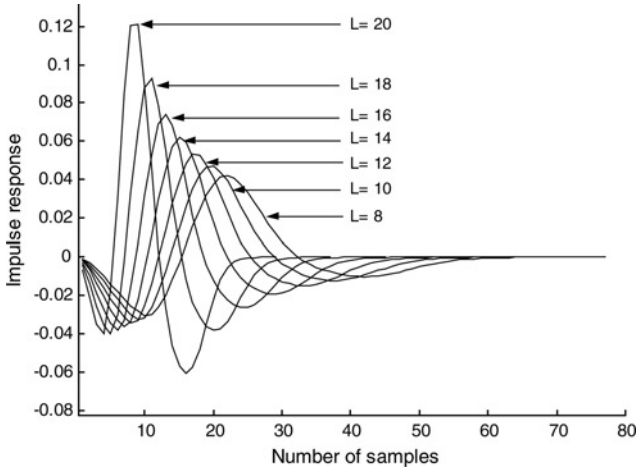

Figure 8 *Impulse responses of the digital band-pass filter for m = 0.68 and different values of L with m = 0.68*

Table 1 Central frequency and 3-dB bandwidth for $m = 0.68$ and different L

Parameter, L	Central frequency, Hz	3-dB bandwidth, Hz
08	18.00	17.27
10	14.40	13.78
12	12.60	11.31
14	10.80	09.66
16	09.00	08.32
18	09.00	07.40
20	07.20	06.44

observation suggests a new dynamical link between fractals and stable physiologic systems. Using the work of Goldberger *et al.*, Sun *et al.* [31] have modelled the His-Purkinje conduction system by a minimum phase fractional order system using the following equation (K is a positive constant)

$$X(s) = \frac{K}{(s^3 + 24\pi s^2 + 192\pi^2 s + 512\pi^3)^{0.7}}$$

3. Approximations of the fractional order operators of (3) and (4) have self-similar structures of the poles and the residues [31].

4. Also, integer order derivatives depend only on the local behaviour of a function, while fractional derivatives depend on the whole history of the function.

3.2 Differentiation, squaring and smoothing

After filtering, the signal has to undergo digital fractional differentiation of order $m = 1.5$ with five samples to provide information about the slope of the QRS complexes. We used fractional order $m = 1.5$ because the authors in [15] stated that the fractional order differentiation for $1 < m < 2$ helps in the detection of inflection points. The differentiated signal will be squared to obtain a positive signal and at the same time this operation will emphasise the higher frequencies of the signal containing the QRS complexes. The squared signal is thus smoothed using an FIR moving average filter truncated by a Blackman window of length N to generate the sequence to be threshold compared (STC) for the R-wave detection. Length N is chosen such that a good compromise is reached between the alteration of the QRS complexes peaks and the attenuation of the P and T peaks and the noise. In our case length N is chosen to be $N = 200$ samples.

4 R-wave detection

Like the proposed band-pass filter, the proposed R-wave detector will also be based on fractional order operators as shown in Fig. 9. After ECG signal pre-processing, the resulting signal is the STC for the R-wave detection. This STC signal is passed through two parallel IIR digital fractional order differentiators of order α and 2α such that $0.5 < \alpha < 1$. The impulse responses of these IIR digital fractional order differentiators are given, respectively, in (14) and (18). The output signals $y1(k)$ and $y2(k)$ of the fractional order differentiators are then used to extract the maximum peaks detected (MPD) as well as their corresponding localisations, which will be classified as R waves. These MPD points are obtained when the signal $y1(k) = 0$ and the signal $y2(k) < 0$. The idea of using fractional order differentiators of order α and 2α comes from the integer order application of the necessary and sufficient conditions for determining the maxima of a function that uses the first and the second derivatives. Besides the differentiation order α was chosen to be $0.5 < \alpha < 1$ in order to have the differentiation order 2α such that $1 < 2\alpha < 2$ because in [15] the authors used a fractional order differentiator whose fractional order was between 1 and 2 to build a fractional order edge detector. They found that this fractional order differentiation-based edge detector improves detection selectivity and provides immunity or robustness to noise.

In the evaluation process the localisations of the R waves detected are compared to the database annotations. The performances of the proposed algorithm were measured in terms of the sensitivity Se and the positive predictivity +P adopted in [29] and [8]. The evaluation parameters Se and +P are defined as

$$\text{Se} = \text{TP}/(\text{TP} + \text{FN}) \tag{23}$$

$$+\text{P} = \text{TP}/(\text{TP} + \text{FP}) \tag{24}$$

where FN (false negative) represents the number of QRS complexes missed and FP (false positive) represents the number of QRS complexes falsely reported. The overall performance achieved by the algorithm is measured in terms of the QRS detection rate defined as [8]

$$\text{QRS detection rate} = \min(\text{Se}, +\text{P}) \tag{25}$$

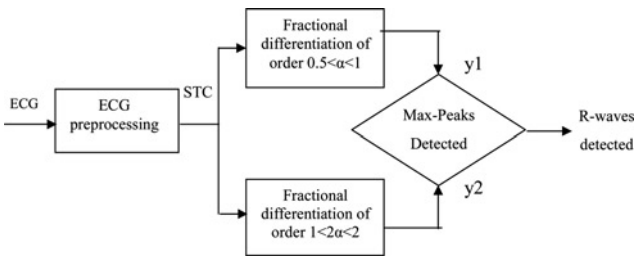

Figure 9 *Block diagram of the R-wave detector*

doi: 10.1049/iet-spr.2008.0094

5 Results evaluation and discussion

The proposed algorithm was implemented on a 3.06-GHz Pentium IV PC using MATLAB version 6.1, and was tested on the ECG signals provided by channel 1 of the MIT/BIH arrhythmia database. The fractional order m of the fractional integration and differentiation, the length L of the fractional digital band-pass filter and the parameter α of the fractional differentiations of orders α and 2α of the detector were set as $(m, L, \alpha) = (0.68, 20, 0.76)$. The average time required for performing our algorithm on each ECG record in the database is about 7 s, which corresponds to around 0.01 ms for each sample.

The waveforms of the different steps of the algorithm using segments from different records are shown in Figs. 10–12. In each of these figures waveforms (a) represent the original ECG signals, Waveforms (b) are the filtered ECG signals using the proposed fractional digital band-pass filter and waveforms (c) represent the sequences to be threshold compared (STC). The outputs of the two fractional order differentiators are represented by waveforms (d) and (e), respectively. The impulses given in (f) correspond to the R waves detected by the proposed algorithm. The MIT/BIH database includes ECG signals with acceptable quality, multiple R-wave peaks, gradual deviation of the baseline and important QRS complex amplitude variations, electric activity of the muscles and QRS complexes with premature ventricular contraction morphology, high noise, high-amplitude P and T waves and patient movement artefacts. Despite all these various morphologies of the QRS complexes and the artefacts contained in the ECG signals of the database, the examples illustrate the capabilities of our algorithm to perform with a high detection rate. The results obtained for 47 records of the standard database are summarised in Table 2.

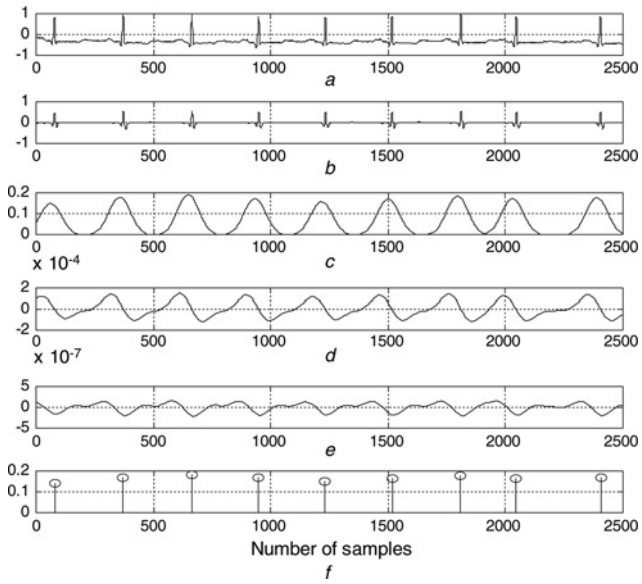

Figure 10 *ECG with an acceptable quality (Record 100)*

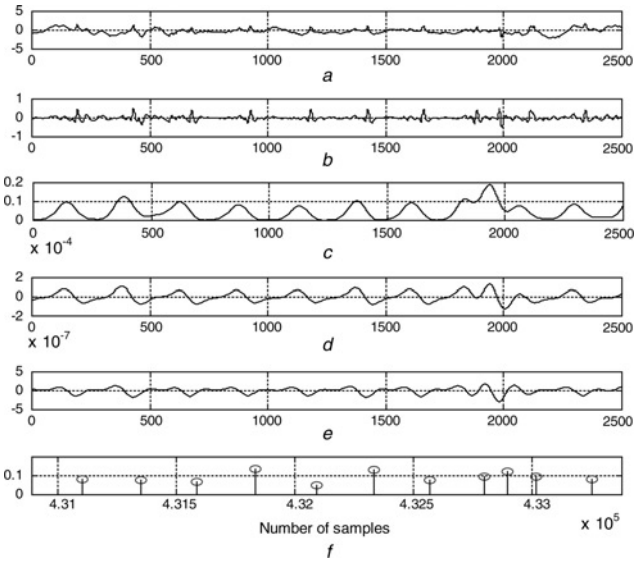

Figure 11 *ECG is highly noisy (Record 105)*

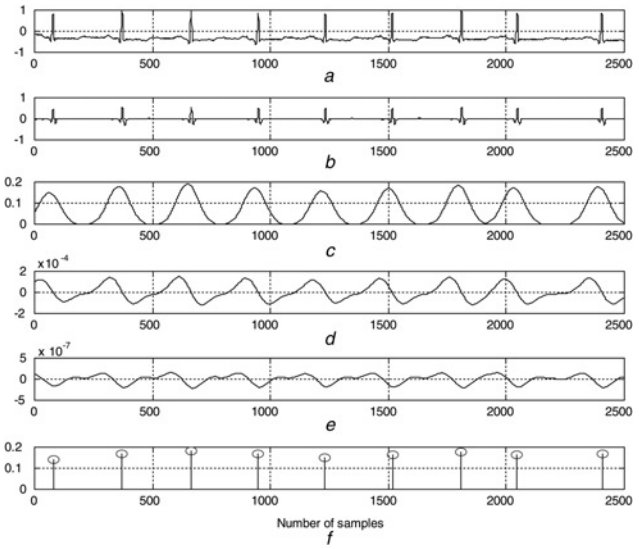

Figure 12 *ECG with uniform PVC (Record 114)*

The proposed algorithm has achieved very good performance on the studied database. It has produced, in total, 153 FPs and 156 FNs, resulting in an overall detection rate of 99.86% with an error of 0.28%. But the individual detection rates of the records vary from 98.70% to 100.00% depending on the quality of the ECG signal. Finally, we compared the performance of our algorithm with six QRS complex detectors reported in the literature. They were all tested on the first channel of the MIT/BIH arrhythmia database. The results of the comparison are given in Table 3. The wavelet transform-based method (WT1) [2] is the most efficient, but it is the

Table 2 Performance evaluation of the proposed R-wave detector using first channel of MIT/BIH database with (m, L, α) = (0.68, 20, 0.76)

Record (number)	TP (beats)	FN (beats)	FP (beats)	Se (%)	+P (%)	Min (Se, +P)
100	2273	0	0	100.00	100.00	100.00
101	1865	2	5	99.89	99.73	99.73
102	2187	0	0	100.00	100.00	100.00
103	2084	0	1	100.00	99.95	99.95
104	2229	1	5	99.96	99.78	99.78
105	2572	15	33	99.42	98.73	98.73
106	2027	0	3	100.00	99.85	99.85
107	2137	3	1	99.86	99.95	99.86
108	1763	6	9	99.66	99.49	99.49
109	2532	0	0	100.00	100.00	100.00
111	2124	1	2	99.95	99.91	99.91
112	2539	0	2	100.00	99.92	99.92
113	1795	0	1	100.00	99.94	99.94
114	1879	0	9	100.00	99.52	99.52
115	1953	0	1	100.00	99.95	99.95
116	2412	19	3	99.22	99.88	99.22
117	1535	0	1	100.00	99.93	99.93
118	2278	0	1	100.00	99.96	99.96
119	1987	0	2	100.00	99.90	99.90
121	1863	1	2	99.95	99.89	99.89
122	2476	0	0	100.00	100.00	100.00
123	1518	0	1	100.00	99.93	99.93
124	1619	0	1	100.00	99.94	99.94
200	2601	3	1	99.88	99.96	99.88
201	1963	11	4	99.44	99.80	99.44
202	2136	3	1	99.86	99.95	99.86
203	2980	39	16	98.71	99.47	98.71
205	2656	2	1	99.92	99.96	99.92
208	2955	16	4	99.46	99.86	99.46
209	3004	0	2	100.00	99.93	99.93
210	2650	22	2	99.18	99.92	99.18
212	2748	0	1	100.00	99.96	99.96
213	3251	1	0	99.97	100.00	99.97
214	2261	1	1	99.96	99.96	99.96
215	3363	0	0	100.00	100.00	100.00

Continued

doi: 10.1049/iet-spr.2008.0094

Table 2 *Continued*

Record (number)	TP (beats)	FN (beats)	FP (beats)	Se (%)	+P (%)	Min (Se, +P)
217	2208	2	4	99.91	99.82	99.82
219	2154	0	2	100.00	99.91	99.91
220	2048	0	0	100.00	100.00	100.00
221	2427	3	1	99.88	99.96	99.88
222	2483	3	3	99.88	99.88	99.88
223	2605	0	1	100.00	99.96	99.96
228	2053	0	14	100.00	99.32	99.32
230	2256	0	1	100.00	99.96	99.96
231	1571	0	1	100.00	99.94	99.94
232	1780	0	10	100.00	99.44	99.44
233	3079	1	0	99.97	100.00	99.97
234	2753	1	0	99.96	100.00	99.96
47 records	107 632	156	153	99.86	99.86	99.86

Table 3 QR detection performance comparison

QRS detector	TP (beats)	FP (beats)	FN (beats)	Error (%)	Se (%)	+P (%)	Min (Se, +P)
This work	**107 632**	**153**	**156**	**0.28**	**99.86**	**99.86**	**99.86**
WT1	116 137	065	112	0.15	99.9	99.94	99.90
FDD	109 492	146	256	0.37	99.76	99.86	99.76
TMP	109 481	137	335	0.42	99.57	99.87	99.57
WT2	102 654	529	459	0.96	99.55	99.49	99.49
BP1	108 889	248	340	0.54	99.68	99.77	99.68
BP2	115 294	507	277	0.68	99.76	99.56	99.56

slowest because the average time required for processing each sample is about 0.4 ms. The fractional digital differentiation-based algorithm (FDD) [3] is very efficient, but it cannot be used for online processing because its proposed FIR band-pass filter is not causal. The detector based on topological mapping parameters (TMP) [4], the two detectors based on classical band-pass filtering (BPI [7] and BPII) [6] and the more recent detector based on moving average incorporating the wavelet denoising-based computing method (WT2) [8] are less efficient. Comparing these results, the proposed algorithm is among the most efficient detectors. The different processing steps proposed require an average processing time of 0.01 ms for each ECG sample with a sampling rate of 360 Hz. This speed is very good compared with the speeds of the WTI and WTII algorithms [2] and [8], respectively.

6 Conclusion

It is now well known that many physical phenomena are modelled accurately and effectively using fractional derivatives, whereas the classical integer derivative-based models capture these phenomena only approximately. Also, integer order derivatives depend only on the local behaviour of a function, while fractional derivatives depend on the whole history of the function. In the last decades, considerable focus on fractional calculus has been simulated by the applications of this concept in different areas of physics and engineering. So, in this paper we present a method for detecting the R wave in the QRS complex of the ECG based on digital differentiation and integration of fractional order. The technique is developed around an FIR band-pass digital filter to suppress the P and T waves and different noises. Then the signal was passed through a non-linear transformation to

enhance the QRS complexes. Finally, a novel R-peak detection method was proposed based on two digital fractional differentiators of order α and 2α such that $0.5 < \alpha < 1$, without using any threshold in the decision rules to determine the R waves of the QRS complexes. The MIT/BIH arrhythmia database is used to test the effectiveness of the proposed method whose performance was evaluated in terms of the detection rate. The numerical results indicated that the method has achieved about 99.86%. The results obtained are also presented, discussed and compared with the most recent and efficient R-wave detection algorithms. Our method also indicates that there might be a degree of flexibility for parameter value selection as well as robustness over a wide range of noise contamination because of the use of these fractional order operators. Besides, all the processing steps of the proposed algorithm are digitally implemented, which lead to an easier real-time implementation.

7 References

[1] FRESEN G.M., JANNETT T.C., JADALLAH M.A., YATES S.L., QUINT S.R., NAGLE H.T.: 'A comparison of the noise sensitivity of nine QRS detection algorithms', *IEEE Trans. Biomed. Eng.*, 1990, **7**, (1), pp. 85–98

[2] ZHENG C., LI C., TAI C.: 'Detection of ECG characteristic points using wavelet transforms', *IEEE Trans. Biomed. Eng.*, 1995, **42**, (1), pp. 21–28

[3] FERDI Y., HERBEUVAL J.P., CHAREF A., BOUCHEHAM B.: 'R wave detection using fractional digital differentiation', *ITBM-RBM*, 2003, **24**, (5), pp. 273–280

[4] LEE J., JEONG K., YOON J., LEE M.: 'A simple real-time QRS detection algorithm'. 18th Ann. Int. Conf. IEEE Eng. Med. Bio. Soc., Amsterdam, 1996, vol. 4, pp. 1396–1398

[5] XUE Q., HU Y.H., TOMKINS W.J.: 'Neural-network-based adaptive matched filtering for QRS detection', *IEEE Trans. Biomed. Eng.*, 1992, **39**, (4), pp. 317–329

[6] PAN J., TOMPKINS W.J.: 'A real-time QRS detection algorithm', *IEEE Trans. Biomed. Eng.*, 1985, **32**, (3), pp. 230–236

[7] HAMILTON P.S., TOMPKINS W.J.: 'Quantitative investigation of QRS detection rules using MIT/BIH Arrhythmia database', *IEEE Trans. Biomed. Eng.*, 1986, **33**, (12), pp. 1157–1165

[8] CHEN S-W., CHEN H-C., CHAN H.-L.: 'A real-time QRS detection method based on moving-averaging incorporating with wavelet denoising', *Comput. Meth. Prog. Biomed.*, 2006, **82**, pp. 187–195

[9] ICHISE M., NAGAYANAGI Y., KOJIMA T.: 'An analog simulation of non-integer order transfer functions for analysis of electrode processes', *J. Electro. Anal. Chem.*, 1971, **33**, pp. 253–256

[10] SUN H.H., ONARAL B.: 'A unified approach to represent metal electrode polarization', *IEEE Trans. Biomed. Eng.*, 1983, **30**, pp. 399–406

[11] TORVIK P.J., BAGLEY R.L.: 'On the appearance of the fractional derivative in the behavior of real materials', *ASME J. Appl. Mech.*, 1994, **51**, pp. 294–298

[12] OUSTALOUP A.: La Dérivation Non Entière: Théorie, Synthèse et Applications. Editions Hermes, 1995

[13] CHEN Y.Q., MOORE K.L.: 'Discretization schemes for fractional-order differentiators and integrators', *IEEE Trans. Cir. Syst.*, 2002, **49**, pp. 363–367

[14] FERDI Y., HERBEUVAL J.P., CHAREF A.: 'Variance reduction of prediction error using fractional digital differentiation: application to ECG signal processing'. Proc. 23rd IEEE/EMBS Annual Conf., Istanbul, Turkey, 2001, pp. 25–28

[15] MATHIEU B., MELCHIOR P., OUSTALOUP A., CEYRAL C.: 'Fractional differentiation for edge detection', *Signal Process.*, 2003, **83**, pp. 2421–2432

[16] GOUTAS A., FERDI Y., HERBEUVAL J-P., BOUDRAA M., BOUCHEHAM B.: 'Digital fractional order differentiation-based algorithm for P and T-waves detection and delineation', *ITBM-RBM*, 2005, **26**, pp. 127–132

[17] SIEROCIUK D., DZIELINSKI A.: 'Fractional Kalman filter algorithm for the states, parameters and order of fractional system estimation', *Int. J. Appl. Math. Comput. Sci.*, 2006, **16**, (1), pp. 129–140

[18] TSENG C-C.: 'Design of variable and adaptive fractional order FIR differentiators', *Signal Process.*, 2006, **86**, (10), pp. 2554–2566

[19] CHAREF A.: 'Analogue realization of fractional order integrator, differentiator and fractional $PI^{\lambda}D^{\mu}$ controllers', *IEE Proc. Control Theory Appl.*, 2006, **153**, (6), pp. 714–720

[20] CHAREF A., SUN H.H., TSAO Y.Y., ONARAL B.: 'Fractal system as represented by singularity function', *IEEE Trans. Automatic Control*, 1992, **37**, (9), pp. 1465–1470

[21] OGATA K.: 'Discrete-time control systems' (Prentice Hall, Englewood Cliffs, USA, 1987)

[22] HAMDAOUI K., CHAREF A.: 'A new discritization method for the fractional order differentiator via bilinear and backward transformations'. Proc. Int. Conf. Modeling and Simulation (MS'07), Algiers, Algeria, 2–4 July 2007

[23] SAHAMBI J.S., TANDON S.N., BHATT R.K.P.: 'Using wavelet transforms for ECG characterization', *IEEE Eng. Med. Biol. Mag.*, 1997, **16**, (1), pp. 77–83

doi: 10.1049/iet-spr.2008.0094

[24] KUNT M., REY H., LIGTENBERG A.: 'Preprocessing of electrocardiograms by digital techniques', *Signal Process.*, 1982, **4**, pp. 215–222

[25] JANÉ R., LAGUNA P., CAMINAL P., RIX H.: 'Adaptive filtering of high-resolution ECG signals'. IEEE Comp. Cardiol. Proc., Chicago, USA, 23–26 September 1990, pp. 23–26

[26] SZILÀGY L., BENYO Z.S., SZILAGYI M., SZLAVECZ A., NAGY L.: 'On-line QRS complex detection using wavelet filtering'. Proc. – 23rd Annual Conf. – IEEE/EMBS, Istanbul, Turkey, 2001, pp. 25–28

[27] SCHUCK JR A., WISBECK J.O.: 'QRS detector pre-processing using the complex wavelet transform'. Proc. 25th Ann. Int. Conf. – IEEE/EMBS Cancun, Mexico, 17–21 September 2003

[28] KOHLER B.-U., HENNIG C., ORGLMEISTER R.: 'The principles of software QRS detection', *IEEE Eng. Med. Biol. Mag.*, 2002, **21**, (1), pp. 42–57

[29] PAHLM O., SÖMMO L.: 'Software QRS detection in ambulatory monitoring – a review', *Med. Biol. Eng. Comput.*, 1984, **22**, pp. 289–297

[30] GOLDBERGER A.L., BHARGAVA V., WEST B.J., MANDEL A.J.: 'On a mechanism of cardiac electrical stability, the fractal hypothesis', *Biophys J.*, 1985, **48**, pp. 525–528

[31] SUN H.H., CHAREF A.: 'Fractal systems: a time domain approach', *Ann. Biomed. Eng.*, 1990, **18**, pp. 597–621